

Original Article

Ginsenoside Rg3 decreases breast cancer stem-like phenotypes through impairing MYC mRNA stability

Jin-Yue Ning^{1*}, Zi-Han Zhang^{2*}, Jia Zhang^{3*}, Yong-Min Liu¹, Guan-Chu Li⁴, A-Man Wang¹, Ying Li¹, Xiu Shan¹, Ju-Hong Wang⁵, Xu Zhang⁶, Yi Zhao¹

¹Department of Oncology, The First Affiliated Hospital of Dalian Medical University, Dalian Medical University, Dalian 116011, Liaoning, China; ²Medical College of Tianjin University, Tianjin 300072, China; ³Department of Oncology, People's Hospital of Ningxiang, Ningxiang 410600, Hunan, China; ⁴National Clinical Research Center for Gynecology and Obstetrics, Tongji Medical College, Tongji Hospital, Huazhong University of Science and Technology, Wuhan 430000, China; ⁵Department of Thoracic Surgery, National Cancer Center/National Clinical Research Center for Cancer/Cancer Hospital, Chinese Academy of Medical Sciences and Peking Union Medical College, Beijing 100021, China; ⁶Department of Thoracic Surgery, The Second Hospital of Dalian Medical University Cardiovascular Hospital, Dalian 116000, Liaoning, China. *Equal contributors.

Received September 16, 2023; Accepted January 28, 2024; Epub February 15, 2024; Published February 28, 2024

Abstract: Breast cancer stem cells (BCSCs) are responsible for breast cancer metastasis, recurrence and treatment resistance, all of which make BCSCs potential drivers of breast cancer aggression. Ginsenoside Rg3, a traditional Chinese herbal medicine, was reported to have multiple antitumor functions. Here, we revealed a novel effect of Rg3 on BCSCs. Rg3 inhibits breast cancer cell viability in a dose- and time-dependent manner. Importantly, Rg3 suppressed mammosphere formation, reduced the expression of stemness-related transcription factors, including c-Myc, Oct4, Sox2 and Lin28, and diminished ALDH(+) populations. Moreover, tumor-bearing mice treated with Rg3 exhibited robust delay of tumor growth and a decrease in tumor-initiating frequency. In addition, we found that Rg3 suppressed breast cancer stem-like properties mainly through inhibiting MYC expression. Mechanistically, Rg3 accelerated the degradation of MYC mRNA by enhancing the expression of the let-7 family, which was demonstrated to bind to the MYC 3' untranslated region (UTR). In conclusion, our findings reveal the remarkable suppressive effect of Rg3 on BCSCs, suggesting that Rg3 is a promising therapeutic treatment for breast cancer.

Keywords: Rg3, breast cancer stem cells, MYC, RNA stability, let7

Introduction

Breast cancer is the most common cancer and the second leading cause of cancer death among women [1]. Despite the development of advanced diagnostic measures and therapeutic methods, including surgery, chemotherapies, hormonal therapies and radiotherapy, a significant portion of patients eventually suffer from tumor relapse [2]. Accumulating evidence suggests that breast cancer stem cells (BCSCs), a population of cells that can self-renew, differentiate and initiate and sustain tumor growth, are responsible for cancer recurrence, drug resistance, and metastasis [3-5]. BCSCs are highly enriched in the CD44^{high}/CD24^{low} subpopulation and are highly expressed aldehyde dehydrogenase enzymes (ALDHs), which have

been shown to be useful biomarkers for cancer stem-like cells [6, 7]. Breast cancer cells were isolated according to the surface marker CD44^{high}/CD24^{low} and exhibited two important characteristics: unlimited self-renewal and the capacity to generate differentiated progeny [8]. Recently, ALDH(+) cells were recognized to contribute to chemotherapeutic resistance and the aggressiveness of malignant tumors [9, 10]. Consistent with our expectations, CD44^{high}/ALDH^{high} cells exhibited greater expression of stem cell-related markers (Sox2, Oct4, and Nanog) than did CD44^{high}/ALDH^{low} cells [11]. In addition, BCSCs can form mammospheres, which are composed of a portion of CD44^{high}/CD24^{low} cells and simultaneously formulate the putative stem cell marker Oct4; these cells can also generate new tumors with only 1×10³ cells

[12]. Therefore, targeting BCSCs is the current therapeutic avenue for the development of anti-cancer treatments.

MYC is one of the most highly amplified genes among different human cancers [13]. An in vitro study of the oncogene Ras revealed that normal embryonic fibroblasts cannot transform into tumor cells unless MYC is present, suggesting that MYC is an oncogene [14]. Canonically, as a common transcription factor, the encoded protein of MYC (Myc) dimerizes with Max and binds target DNA sequences or E boxes (with the sequence 5'-CANNTG-3') to regulate the transcription of genes involved in tumor growth and proliferation [15, 16]. Another critical mode for Myc-mediated regulation is the influence of widespread miRNAs [17]. For instance, Myc can directly bind to miR-17 cluster intron 1, which has the E-box sequence CACGTG, to regulate miR-17 expression [18]. Interestingly, MYC is also affected by miRNAs (let-7, miR-34, and miR-145), resulting in post-translational modulation of MYC [19-21]. In addition to its role in tumorigenesis, MYC was identified as one of four Yamanaka factors, including Sox2, Oct4, and Klf4, that can collectively reprogram fibroblasts to a pluripotent stem cell state [22, 23]. Considering that MYC lies at the crossroads of many growth-promoting signal transduction pathways, targeting MYC to inhibit cancer progression could be an effective treatment.

Ginsenosides, major active pharmaceutical ingredients in the traditional medicine ginseng, have been gradually reported to have antitumor effects on multiple cancers, such as lung cancer, gastric cancer and human melanoma [24-26]. Rg3, a monomer extracted from ginseng, has received extensive attention in tumor treatment. Rg3 downregulated fucosyltransferase 4 (FUT4)-mediated EGFR inactivation and blocked the MAPK and NF- κ B signaling pathways. These properties could inhibit the epithelial-mesenchymal transition (EMT) capacity of lung cancer cells [27]. In addition, Rg3 treatment induces breast cancer cell apoptosis by blocking NF- κ B signaling, reducing the activation of ERK and Akt and destabilizing mutant p53 [28]. Moreover, Rg3 has been reported to attenuate the phosphorylation cascade of VEGF-dependent p38/ERK signaling and inhibit VEGF-dependent tumor angiogenesis [29]. Importantly, Rg3 inhibited doxorubicin-induced protective autophagy in hepatocellular carcinoma (HCC), which

sensitizes HCC to doxorubicin [30]. An in vivo experiment showed that Rg3 combined with gemcitabine significantly improved the survival and quality of life of tumor-bearing mice [31]. These studies suggest that Rg3 could be a potential therapeutic agent for different kinds of tumors.

In the present study, we demonstrated that Rg3 inhibited breast cancer cell viability in vitro and in vivo. Importantly, we found that the application of Rg3 could reduce BCSC maintenance, mainly through downregulating MYC mRNA. Mechanistically, Rg3 could destabilize MYC by enhancing the expression of the let-7 family. These results suggested the potential use of Rg3 in breast cancer treatment by targeting BCSCs.

Materials and methods

Reagents and cell culture

20 (R)-Rg3 was obtained from Dalian Fusheng Pharmaceutical Company (Fusheng, Dalian, China). Rg3 was dissolved in serum-free culture medium to the required concentration for in vitro study and in saline for in vivo study and then filtered through a 0.22 μ m sterile membrane. All cell lines (MDA-MB-231, MCF-7, SK-BR-3, BT-549 and HEK293T) were purchased from American Type Culture Collection (ATCC; Manassas, VA, USA). MDA-MB-231, MCF-7, SK-BR-3 and HEK293T cells were maintained in Dulbecco's modified Eagle's medium (DMEM, Invitrogen) supplemented with 10% fetal bovine serum (Gibco). BT-549 cells were maintained in RPMI-1640 (Invitrogen) supplemented with 10% fetal bovine serum (Gibco). All the cells were incubated at 37°C in a humidified incubator containing 5% CO₂.

Cell viability assay

The cells were seeded in 96-well microplates (1 \times 10⁴ cells/well in 100 μ L) in an incubator at 37°C with 5% CO₂. When the confluency of the cells reached 80%, the medium was replaced with RPMI 1640 containing 2% FBS, and the cells were cultured for 24 h. Then, 10 μ L of CCK-8 reagent was added to each well, and the cells were cultured for another 2 h. The optical density at 450 nm was calculated by a microplate reader (Varioskan Flash 3001, Thermo Fisher Scientific, Waltham, USA) every hour to determine the best culture time.

Rg3 impairs MYC mRNA stability to inhibit breast cancer stemness

Table 1. The sequences of primers used in quantitative PCR

Gene name	Forward primer 5'→ 3'	Reverse primer 5'→ 3'
ACTB	ATCAAGATCATTGCTCCTCCTGAG	CTGCTTGCTGATCCACATCTG
MYC	CGAGGAGGAGAACTTCTACCAGC	CGAGAAGCCGCTCCACATACAGTCC

Mammosphere formation assay

Dissociated single cells (1×10^3) were seeded in 6-well ultralow attachment plates (Corning). The cells were cultured in serum-free DMEM/F-12 medium (Gibco) supplemented with 20 ng/ml epithelial growth factor (EGF, Sigma), 20 ng/ml basic fibroblast growth factor (bFGF, BD Biosciences) and 2% B27 (Invitrogen) in the absence and presence of 20 (R)-Rg3 for two weeks. All spheroids were photographed by an inverted microscope (Olympus, Japan). The number and diameter of the spheroids were calculated by using spheres greater than 50 μm in diameter. The spheroids were collected by centrifugation, after which RNA was extracted and western blotting was performed.

Real-time quantitative PCR (RT-qPCR)

The qualified postdetection RNA samples were added to HiScript III RT SuperMix (+gDNA wiper) (Novozymes, China) for qRT-PCR to perform reverse transcription. The sequences of primers used are shown in **Table 1**. The results were analyzed by the Ct comparison method ($2^{-\Delta\Delta Ct}$) to calculate the relative expression of the genes.

Western blotting

After isolation, the protein concentration was quantified using a BCA Protein Assay Kit (Bio-Rad, USA). After separation by SDS-polyacrylamide gel electrophoresis, the proteins were transferred to a PVDF membrane (Millipore, USA). Subsequently, the membranes were blocked with 5% skim milk and incubated with primary antibodies for 24 h at 4°C. Then, the membrane was incubated with the appropriate HRP-conjugated secondary antibody and visualized using an ECL detection kit. ImageJ software was used to analyze the results.

Clinical samples and primary breast cancer cell isolation

All breast cancer tissues were obtained. The breast cancer tissues were kept in liquid nitro-

gen for protein extraction. For mouse xenograft cancer cell isolation, the tumor xenografts were mechanically and enzymatically dissociated to yield clumps of epithelial cells by incubation at 37°C for 2 hours in a 1:1 solution of collagenase I (3 mg/mL):hyaluronidase (100 U/mL; Sigma). After filtration through a 40 μm pore filter (BD Biosciences) and washing with PBS, the cells were cultured in DMEM (Invitrogen) supplemented with 10% fetal bovine serum (Gibco).

Xenograft tumor formation and detection of potential toxicological effects

All animal studies were approved by the Institute Animal Care and Use Committee of Dalian Medical University and were carried out in accordance with established institutional guidelines and approved protocols. For the xenograft transplantation assay, female BALB/c nude mice (4-6 weeks old) were purchased from Beijing Vital River Laboratory Animal Technology Co., Ltd., and housed in a specific pathogen-free (SPF) environment. The mice were acclimatized for one week before being used for experiments. MDA-MB-231 cells (1×10^6) in PBS containing 50% Matrigel (BD Biosciences) were subcutaneously injected into the right flank of the mice. One week after injection, the tumor-bearing mice were randomly divided into Rg3 and control groups ($n = 5$ per group). Rg3 (10 mg/kg body weight) was administered to mice every two days for 3 weeks via intraperitoneal injection, whereas the control group received normal saline only. The body weights of the animals and the two perpendicular diameters (a and b) were recorded every 3 days. Tumor volume (V) was calculated according to the following formula: $V = (a \times b^2)/2$. After 4 weeks, the tumor mass was resected and dissociated into individual cancer cells. Then, 1×10^6 , 1×10^5 , 1×10^4 or 1×10^3 tumor cells isolated from the primary tumor xenografts were injected into female BALB/c nude mice (4-6 weeks old). The subsequent steps were similar to those of the first tumor transplantation. To detect potential toxicological effects, C57BL/6J

Rg3 impairs MYC mRNA stability to inhibit breast cancer stemness

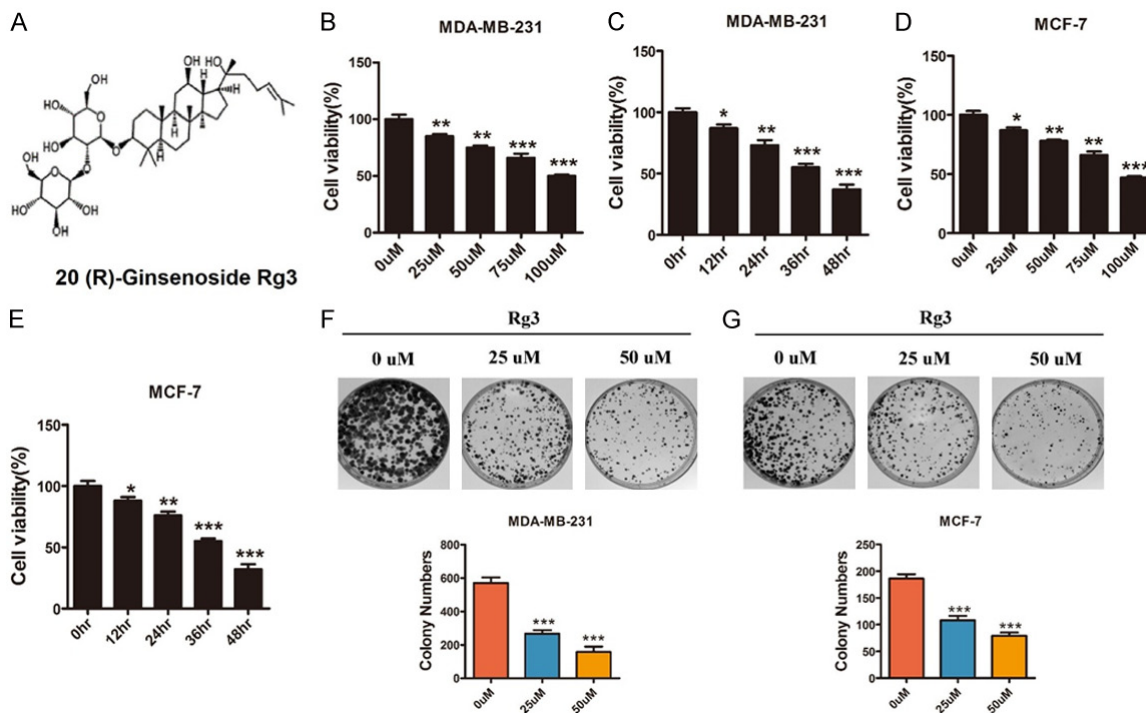


Figure 1. Rg3 inhibits breast cancer cell growth. (A) Structure of 20 (R)-ginsenoside Rg3. (B) MDA-MB-231 cells were treated with Rg3 (0 μ M, 25 μ M, 50 μ M, 100 μ M) for 48 h. Cell viability was determined by a CCK-8 assay as described in the Materials and Methods. (C) MDA-MB-231 cells were treated with 50 μ M Rg3 for 0 h, 12 h, 24 h, 36 h, or 48 h. Cell viability was determined by a CCK-8 assay. (D) MCF-7 cells were treated with Rg3 (0 μ M, 25 μ M, 50 μ M, 100 μ M) for 48 h. Cell viability was determined by a CCK-8 assay. (E) MCF-7 cells were treated with 50 μ M Rg3 for 0 h, 12 h, 24 h, 36 h, or 48 h. Cell viability was determined by a CCK-8 assay. (F) Plate colony formation was analyzed following treatment with different concentrations of Rg3 (0 μ M, 25 μ M, 50 μ M) in MDA-MB-231 cells and (G) MCF-7 cells. The data are presented as the mean \pm SD of three independent experiments. Comparisons were analyzed by two-tailed Student's *t* tests. **P* < 0.05, ***P* < 0.01, ****P* < 0.001.

mice were treated with Rg3 (10 mg/kg, every three days) for three weeks, after which mouse weight was subsequently measured. The investigation was conducted in accordance with ethical standards and according to the Declaration of Helsinki and according to national and international guidelines.

Statistical analysis

Statistical analysis of the results was performed by using GraphPad Prism software. All the data are presented as the mean \pm SD. Two-tailed Student's *t* tests were used for two-group comparisons, and one-way ANOVA was used for multiple-group comparisons. **P* < 0.05 was considered to indicate statistical significance.

Results

Rg3 inhibits human breast cancer cell viability

The structure of Rg3 is shown in **Figure 1A**. To determine the antitumor effect of Rg3 on

breast cancer, MDA-MB-231, MCF-7 and SK-BR-3 cells were treated with different concentrations of Rg3 (from 0 to 100 μ M) for 48 hours or the same concentration (50 μ M) for different durations (12 hours, 24 hours, 36 hours and 48 hours). Cell viability was determined by a CCK8 assay. As shown in **Figure 1B-E** and **Supplementary Figure 1A, 1B**, Rg3 significantly decreased cell viability in a dose- and time-dependent manner in breast cancer cells. Then, we performed colony formation assays to detect the anti-clonogenicity ability of Rg3. After treatment with different concentrations of Rg3 (0, 25 and 50 μ M), the colony numbers were distinctly decreased in breast cancer cells in a dose-dependent manner compared with those after solvent treatment (**Figure 1F, 1G, Supplementary Figure 1C**). Notably, Rg3 had little effect on the viability of mammary epithelial MCF-10A cells (**Supplementary Figure 1D and 1E**). These data indicated that Rg3 has a cytotoxic effect on breast cancer cells and inhibits cell growth.

Rg3 impairs MYC mRNA stability to inhibit breast cancer stemness

Rg3 suppresses stem-like properties in breast cancer cells

To determine whether Rg3 inhibits BCSCs, we first performed mammosphere-forming assays. As shown in **Figure 2A**, the number and size of the mammospheres were significantly reduced after Rg3 treatment in the MDA-MB-231 cells. Consistently, compared with those in the control groups, the sphere formation ability of MCF-7 cells that received different concentrations of Rg3 was apparently suppressed (**Figure 2B**). Furthermore, by western blot, we revealed that Rg3 decreased the expression of self-renewal-related factors, such as c-Myc, Oct4, Sox2, and Lin28, in breast cancer cells (**Figure 2C, 2D**). However, these proteins were also inhibited by Rg3 in a time-dependent manner (**Supplementary Figure 2A, 2B**). Consistent with these findings, immunofluorescence assays revealed decreased expression of c-Myc, Oct4, Sox2, and Lin28 after Rg3 treatment (**Supplementary Figure 2C**). High expression of ALDH has been used as a unique reporter of stem cell activity in the mammary gland [6]. Therefore, we used flow cytometry analysis to determine the proportions of ALDH(+) subpopulation breast cancer cells. As shown in **Figure 2E** and **Supplementary Figure 2D**, after 3 days of Rg3 (25 μ M) treatment, the ALDH(+) population of MDA-MB-231 cells was dramatically reduced from 9.4% to 2.9% ($P < 0.05$). Similarly, the ALDH(+) subpopulation in MCF-7 cells decreased from 4.8% to 2.4% after culture with Rg3 (**Figure 2F, Supplementary Figure 2E**). Collectively, these results revealed that Rg3 has the potential to inhibit BCSC properties.

Rg3 delays tumor growth and abrogates tumor-initiating frequencies in vivo

Given that Rg3 diminishes BCSC properties in vitro, we then examined whether Rg3 affects tumor growth and the tumor-initiating potential of breast cancer cells in vivo. An equal number of MDA-MB-231 cells (1×10^6 cells per mouse) were subcutaneously injected into 4- to 6-week-old female nude mice. When the tumors developed for 7 days, the mice were randomly assigned to receive an intraperitoneal injection of Rg3 (10 mg/kg body weight, every other day) or a saline control. After 3 weeks of treatment, the tumors in the Rg3-treated group (referred to as Rg3) were smaller than those in the con-

trol group (referred to as NS) (**Figure 3A, 3B**). Importantly, body weight did not obviously differ between the Rg3-treated group and the control group (**Figure 3C**). Notably, there was no obvious difference in body weight between the Rg3-treated group and the control group of healthy mice (**Figure 3D**). These findings indicated that tumor growth in xenograft models was significantly suppressed by Rg3, which has favorable toxicological side effects. Furthermore, we isolated cells from xenograft tumors in both the Rg3 group and the control group. Then, we evaluated the expression of stemness-related factors and the colony-forming capacity. As shown in **Figure 3E** and **3F**, compared with control xenograft cells, Rg3-treated cells (referred to as Rg3 cells) exhibited reduced expression of cancer stem-related proteins (c-Myc, Oct4, Sox2, and Lin28) and impaired mammosphere-forming efficiency (referred to as NS cells). Next, a serial transplantation assay was performed in nude mice. Equal amounts of cells (1×10^6 , 1×10^5 , 1×10^4 and 1×10^3) were subcutaneously inoculated into four different flanks of each mouse ($n = 5$) and monitored for 4 weeks. Rg3 treatment significantly impeded secondary limited dilution tumor transplantation compared to that in the saline control group (**Figure 3G**). These results demonstrated that, compared with that in the saline control group, the frequency of secondary tumor xenografts was lower in the Rg3-treated group.

Rg3 impairs breast cancer stem-like properties mainly through suppressing MYC

Since MYC plays a key role in cancer stemness maintenance [32, 33], we next validated the expression of c-Myc in several breast cell lines. The results showed that c-Myc was expressed at low levels in luminal breast cancer cells but was highly expressed in basal breast cancer cells; these cells are mostly regarded as BCSCs (**Figure 3H**). Furthermore, we collected 3 pairs of breast cancer tissues and adjacent normal tissues and performed western blotting to analyze c-Myc expression. The results showed that all the breast cancer tissues presented higher c-Myc levels than did the adjacent normal tissues (**Figure 3I**). To determine whether Rg3 restricts BCSCs by decreasing MYC expression, we cultured breast cancer cells in normal sphere-forming media or media supplemented

Rg3 impairs MYC mRNA stability to inhibit breast cancer stemness

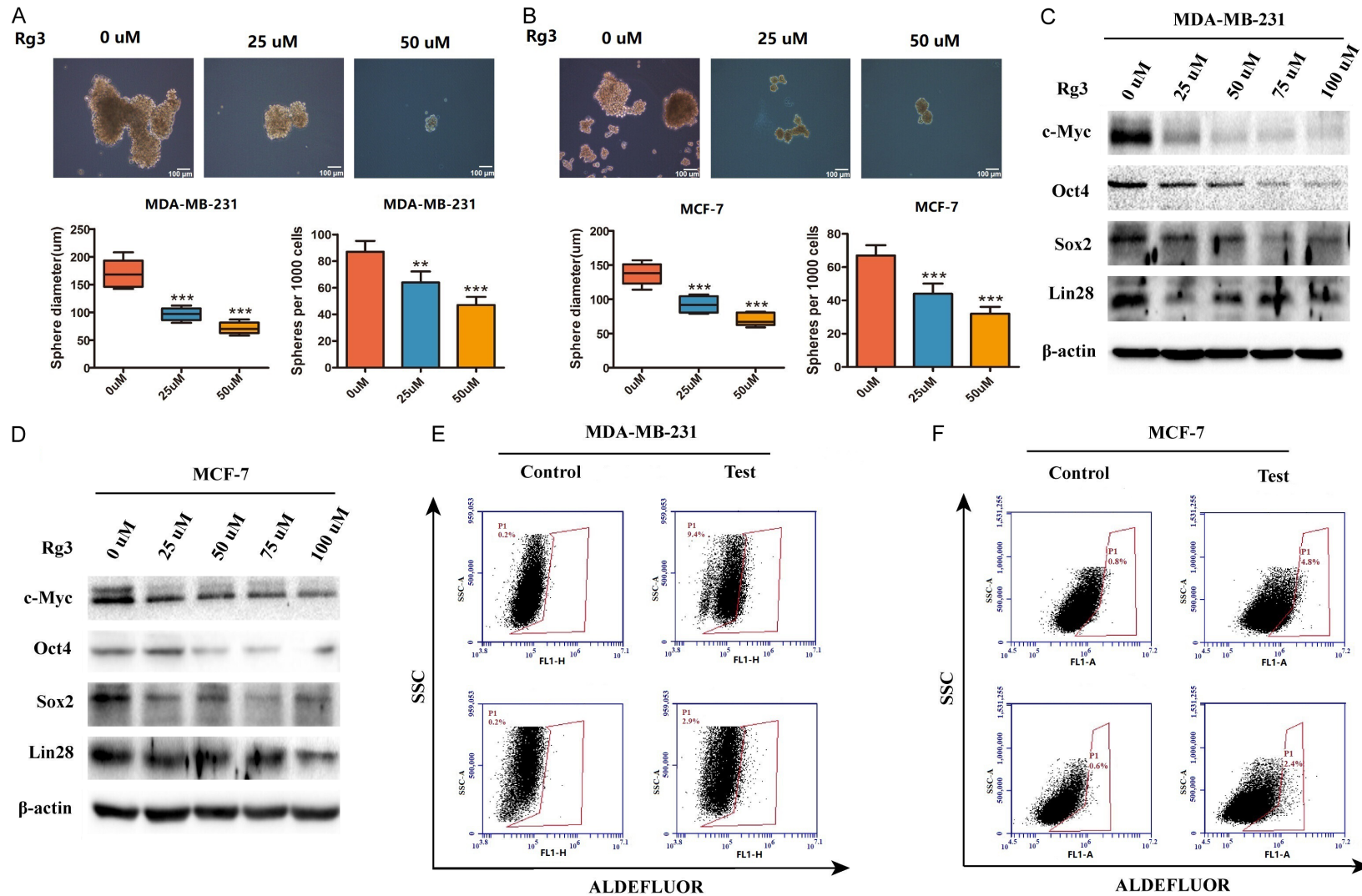


Figure 2. Rg3 attenuates breast cancer cell stem-like properties. (A) The mammosphere-forming abilities of MDA-MB-231 and (B) MCF-7 cells were analyzed following treatment with different concentrations of Rg3 (0 μ M, 25 μ M, 50 μ M). (C) The expression of proteins (c-Myc, Oct4, Sox2, Lin28) was analyzed in MDA-MB-231 cells and (D) MCF-7 cells treated with different concentrations of Rg3 (0 μ M, 25 μ M, 50 μ M, 75 μ M, 100 μ M) by western blot. (E) ALDH-positive populations in MDA-MB-231 cells and (F) MCF-7 cells treated with different concentrations of Rg3 (0 μ M, 25 μ M). NC indicates the negative control. The data are presented as the mean \pm SD of three independent experiments. Comparisons were analyzed by two-tailed Student's t tests. * P < 0.05, ** P < 0.01, *** P < 0.001. Scale bars, 100 μ m.

Rg3 impairs MYC mRNA stability to inhibit breast cancer stemness

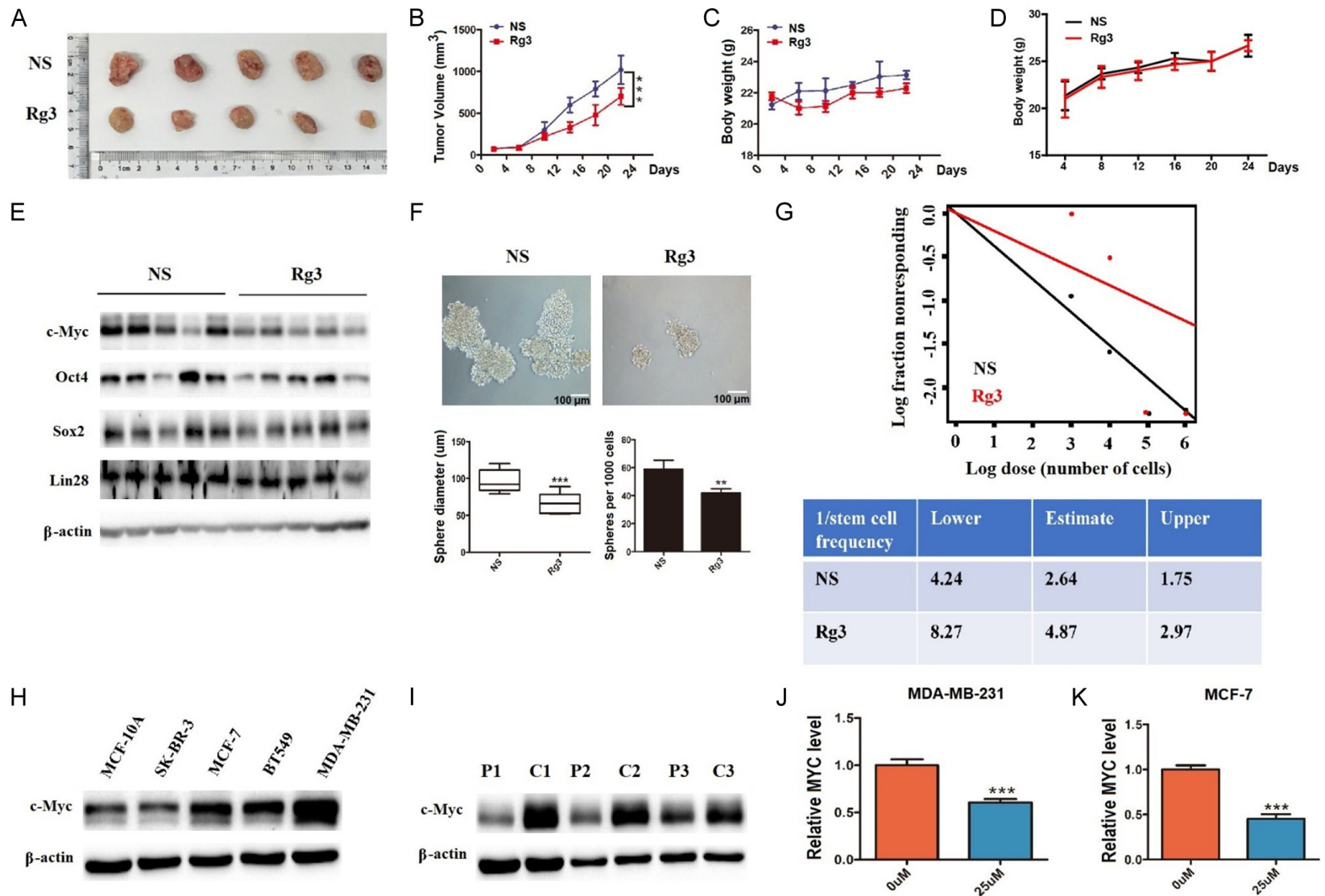


Figure 3. Rg3 impairs the tumor-initiating ability of breast cancer cells in vivo. (A) MDA-MB-231 cells (1×10^6 cells per mouse) were inoculated into the flanks of nude mice. When the tumors developed for 2 days, the mice were randomly assigned to receive Rg3 (10 mg/kg body weight, every other day) or the saline control. Tumor xenografts were monitored for 3 weeks. Tumor volumes were monitored as described in the Materials and methods section. (B) Tumor growth curves are presented as a line chart. (C) The body weights of the mice are presented in the line chart. (D) The body weights of healthy mice are shown in the line chart. (E) The expres-

Rg3 impairs MYC mRNA stability to inhibit breast cancer stemness

sion of proteins (c-Myc, Oct4, Sox2, and Lin28) in different tumors (NS or Rg3) was analyzed via western blotting. (F) Isolated tumor cells from different tumors (NS or Rg3) were plated in low-serum nonadherent culture conditions. Mammosphere-forming abilities were also analyzed. (G) Left: ELDA was performed on isolated tumor cells with or without Rg3 treatment (NS or Rg3) from different tumors subcutaneously inoculated into nude mice. Right: Stem cell frequencies were estimated as the ratio $1/x$ with the upper and lower 95% confidence intervals, where 1 = stem cell and x = all cells. NS represents the saline control. (H) c-Myc expression in different breast cancer cells was analyzed by western blotting. (I) c-Myc expression in three pairs of breast tumor (T) and adjacent normal tissue (P) samples was subjected to western blot analysis. (J) Expression of MYC mRNA was analyzed by RT-qPCR after culture of MDA-MB-231 cells and (K) MCF-7 cells with Rg3. The data are presented as the mean \pm SD of three independent experiments. Comparisons were analyzed by two-tailed Student's *t* tests. **P* < 0.05, ***P* < 0.01, ****P* < 0.001. Scale bars, 100 μ m.

with a low concentration of Rg3 (25 μ M). After two weeks of culture, the MYC mRNA levels were lower in the MDA-MB-231 and MCF-7 cells treated with Rg3 than in the cells treated with solvent (**Figure 3J** and **3K**). Therefore, we hypothesized that MYC might be a main downstream target through which Rg3 decreases the stem-like properties of breast cancer cells. To verify this hypothesis, we used short hairpin RNA (shRNA) to suppress MYC expression in MDA-MB-231 and MCF-7 cells. As shown in **Figure 4A**, MYC was effectively depleted by two different shRNAs. As expected, the sphere formation efficiency was dramatically reduced upon MYC depletion, as indicated by a decrease in both spheroid number and diameter (**Figure 4B**, **4C**). However, in cells depleted of MYC simultaneous and treated with Rg3, little change in sphere formation efficiency was observed (**Figure 4B**, **4C**). Consistently, the colony numbers were markedly decreased following the depletion of MYC by shRNAs in both the MDA-MB-231 and the MCF-7 cells, which exhibited a slight difference after Rg3 treatment (**Supplementary Figure 3A**, **3B**). To further explore the role of Rg3 in MYC-mediated functions, we ectopically overexpressed MYC in both MDA-MB-231 and MCF-7 cells (**Figure 4D**). As reported before, MYC overexpression effectively enhanced mammosphere-forming ability, while Rg3 treatment reversed this increase (**Figure 4E**, **4F**). Consistent with these findings, MYC-upregulated MDA-MB-231 and MCF-7 cells exhibited significantly increased colony formation capacity, whereas treatment with Rg3 suppressed colony formation to a comparative level in cells infected with the empty vector and then treated with Rg3 (**Supplementary Figure 3C**, **3D**). Taken together, these results indicated that Rg3 reduces breast cancer stem-like properties mainly through downregulating MYC expression.

Rg3 decreases MYC mRNA stability by promoting let-7 family expression

To determine the mechanism underlying the decrease in MYC expression, we first assumed that Rg3 may affect the transcription of MYC. We cloned the full sequence of the MYC promoter by PCR and inserted it into the luciferase reporter pGL3-basic plasmid. Dual-luciferase reporter results showed that firefly luciferase activity did not significantly change after Rg3 treatment in either MDA-MB-231 (**Supplementary Figure 4A**) or MCF-7 cells (**Supplementary Figure 4B**), suggesting that Rg3 does not influence MYC transcriptional activity. Then, we treated the cells with actinomycin D (ACTD) to block de novo mRNA synthesis, and total RNA was isolated at the indicated time points (0, 30, 60 and 90 min) after ACTD application. As shown in **Figure 5A-D**, the half-life of MYC mRNA was markedly decreased when cells were treated with Rg3. Consistently, the mRNA level of MYC was significantly reduced by Rg3 treatment for 72 h (**Figure 5E**). Since the let7 family can bind to MYC mRNA and lead to MYC degradation via the RISC complex [19], we then detected whether Rg3 destabilizes MYC mRNA through regulating let7. Indeed, RT-qPCR analysis of the let7 cluster (let7a, let7b, let7c, let7e, let7f, let7g, and let7i) after treatment with Rg3 showed that the let7 cluster was significantly promoted by Rg3 in MDA-MB-231 and MCF-7 cells (**Figure 5F** and **5G**). Furthermore, RAS and DICER, which are direct targets of let7 [34, 35], were detected after Rg3 treatment. As shown in **Supplementary Figure 4C** and **4D**, the expression of DICER and RAS was markedly lower in breast cancer cells cultured with Rg3 than in those cultured with saline. As highly changed members, let7a and let7b were chosen to be delegates of the let7 family. Consistent with the findings of previous reports, transfection with let7a and let7b inhibitors (ilet7) significantly

Rg3 impairs MYC mRNA stability to inhibit breast cancer stemness

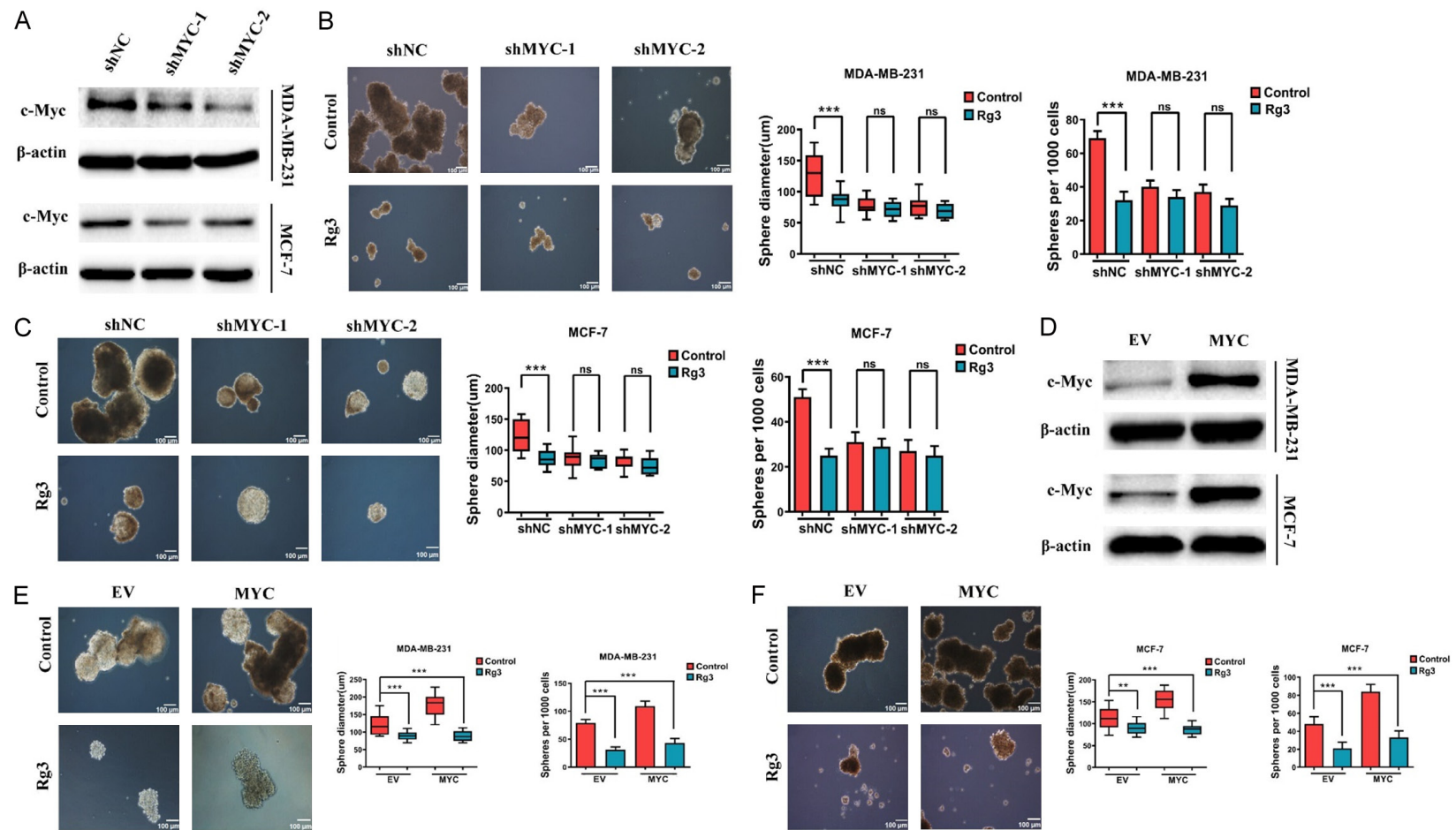


Figure 4. Rg3 inhibits the stem-like properties of breast cancer cells through decreasing MYC levels. (A) The efficiency of MYC knockdown was tested by western blot analysis in MDA-MB-231 cells (top) and MCF-7 cells (bottom). (B) Comparisons of mammosphere-forming abilities were performed following decreases in MYC expression in MDA-MB-231 cells and (C) MCF-7 cells. (D) MYC overexpression efficiency was tested by western blot analysis in MDA-MB-231 cells (top) and MCF-7 cells (bottom). (E) Comparisons of mammosphere-forming abilities were performed after MYC expression was increased in MDA-MB-231 cells and (F) MCF-7 cells. The data are presented as the mean \pm SD of three independent experiments. Comparisons were analyzed by two-tailed Student's t tests. * $P < 0.05$, *** $P < 0.01$, *** $P < 0.001$. Scale bars, 100 μ m.

Rg3 impairs MYC mRNA stability to inhibit breast cancer stemness

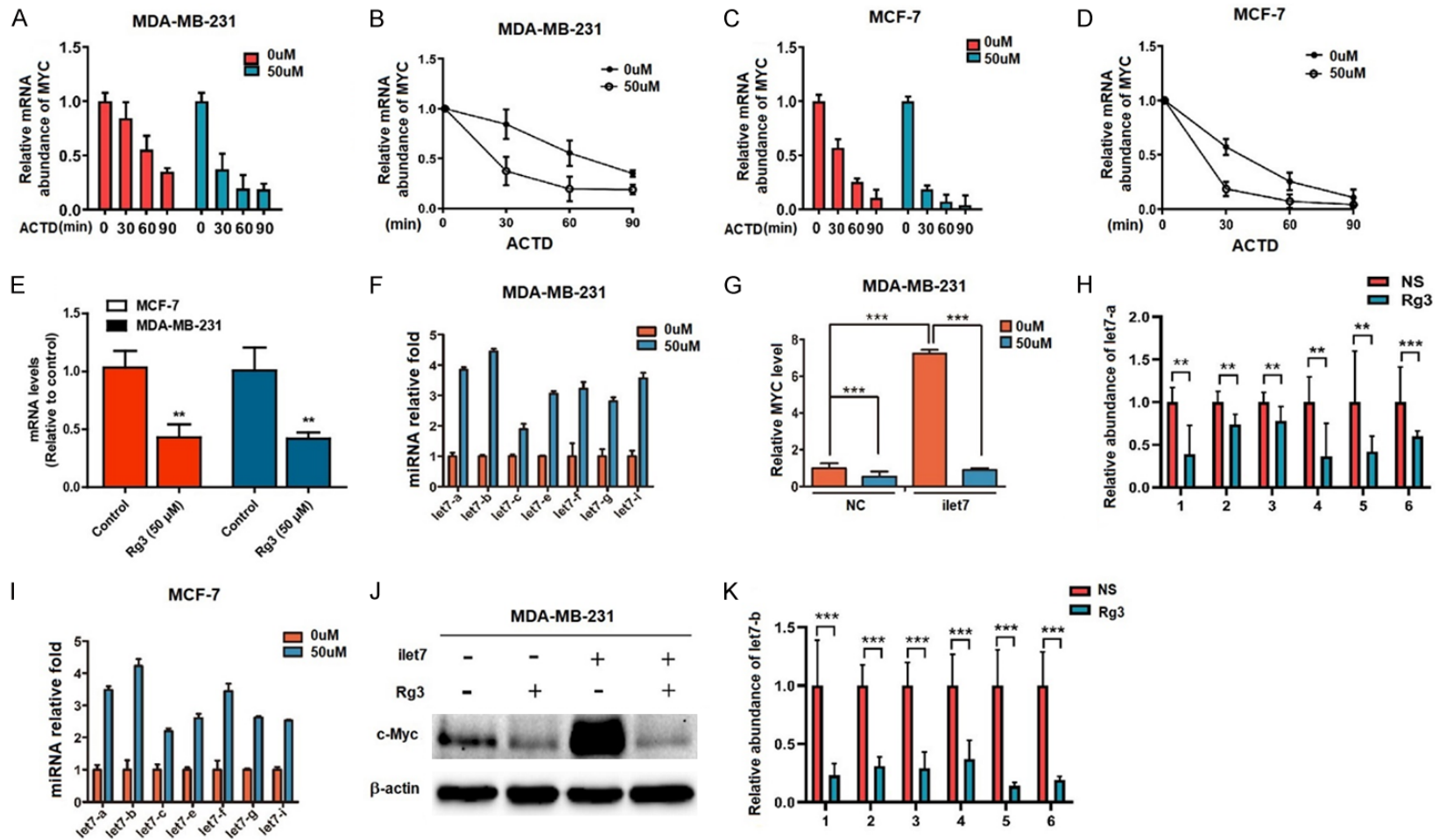


Figure 5. Rg3 upregulates let7 to impair MYC mRNA stability. (A, B) MDA-MB-231 cells and (C, D) MCF-7 cells were treated with or without Rg3 and then cultured with actinomycin D (ACTD, 5 μ g/ml) to block de novo mRNA synthesis, after which total RNA was detected at the indicated time points (0, 30, 60 and 90 min) after ACTD application. (E) The mRNA level of MYC was measured in breast cancer cells treated with or without Rg3. (F) Expression of the let-7 cluster was analyzed by RT-qPCR (RNU6-2 was used as an internal control) after Rg3 treatment in MDA-MB-231 cells and (I) MCF-7 cells. (G) MDA-MB-231 cells were treated with the let-7a/b inhibitor with or without Rg3. The relative MYC concentration was measured by RT-qPCR. (J) The protein expression of c-Myc was measured by western blot. (H) Expression of let-7a and let-7b (K) was analyzed by RT-qPCR in isolated tumor cells from different tumors (NS or Rg3). The data are presented as the mean \pm SD of three independent experiments. Comparisons were analyzed by two-tailed Student's t tests. * $P < 0.05$, ** $P < 0.01$, *** $P < 0.001$.

Rg3 impairs MYC mRNA stability to inhibit breast cancer stemness

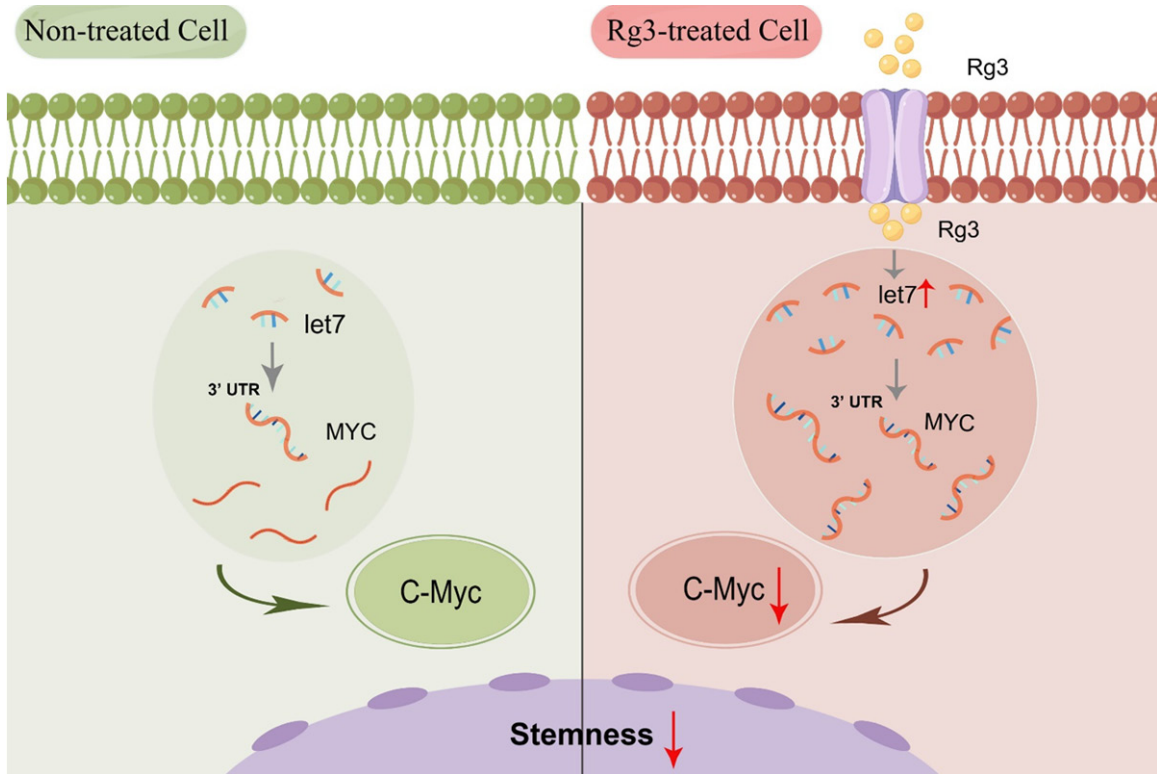


Figure 6. Schematic of the antistemness mechanism of Rg3. Under normal conditions, the let7 family is expressed at low levels in cancer cells, resulting in stable MYC mRNA expression and high c-Myc expression. However, Rg3 treatment upregulated the let-7 cluster, impaired MYC mRNA stability, reduced c-Myc expression and inhibited breast cancer stem-like properties.

promoted MYC expression in both MDA-MB-231 and MCF-7 cells, which was reversed by Rg3 treatment (Figure 5H and 5I, Supplementary Figure 4E and 4F). More importantly, we found that, compared with those in saline-treated mice, let7a and let7b expression in mouse xenograft tumors was dramatically lower after intraperitoneal injection of Rg3 (Figure 5J and 5K). Taken together, these results suggest that Rg3 regulates MYC mRNA stability by promoting the microRNA let-7 cluster.

Discussion

The current study provides compelling evidence that ginsenoside Rg3, derived from ginseng, exerts time- and dose-dependent inhibitory effects on the viability and clonogenicity of breast cancer cells. Importantly, our findings suggest the potential use of Rg3 as an anticancer agent for breast cancer therapy. Rg3 suppressed mammosphere formation, reduced the expression of stem cell-related factors (c-Myc, Oct4, Sox2, and Lin28), and decreased the ALDH(+) subpopulation. Additionally, in vivo

experiments revealed that Rg3 inhibited xenograft tumor volume and tumor-initiating frequency in nude mice. Notably, Rg3 was identified as an accelerator of MYC mRNA degradation, as illustrated in Figure 6.

The primary chemical agents employed in breast cancer treatment, anthracyclines and taxanes, target cancer cell replication through DNA insertion and induce cell cycle arrest, respectively [36, 37]. Despite the positive responses observed with drugs such as trastuzumab, which targets HER2-positive breast cancer, limitations in efficacy and strong side effects remain challenges in contemporary antitumor treatments [38-40]. Recently, traditional drugs, including Rg3 found in the CFDA-approved Shen-Yi capsule, have shown promise in overcoming these challenges. Notably, Rg3 has been utilized as an anti-lung cancer drug in clinical settings, demonstrating its positive impact on patient immunity and quality of life [41]. Our experimental evidence further supports the antitumor potential of Rg3, revealing its ability to inhibit tumor growth and

Rg3 impairs MYC mRNA stability to inhibit breast cancer stemness

angiogenesis in human breast infiltrating duct carcinoma in nude mouse xenotransplantation assays compared to those in the control group (0.5% sodium carboxymethyl cellulose) [42]. Additionally, our innovative experiment demonstrated that the combination of Rg3 with Endostar (a recombinant human endostatin) had stronger antitumor effects on breast cancer-bearing mice than did either drug alone, resulting in lower expression of vascular endothelial growth factor (VEGF) and matrix metalloproteinase (MMP) [43]. Consistent with these studies, our research confirmed that Rg3 can effectively suppress breast cancer cell viability in a time- and dose-dependent manner (**Figure 1B-E**, [Supplementary Figure 1A](#) and [1B](#)). Moreover, Rg3 significantly reduced colony formation ability in breast cancer cells (**Figure 1F**, **1G**, [Supplementary Figure 1C](#)), inspiring confidence in further exploration of the antitumor mechanisms of Rg3.

The ultimate therapeutic effect on patients with breast cancer depends on the duration of recurrence after treatment with different therapeutic strategies. Among multitudinous factors, BCSC populations are considered promising therapeutic targets for breast cancer treatment because of their contributions to tumor relapse and drug resistance [44]. Indeed, breast cancer cells that were resistant to epirubicin contained high CD44^{High}/CD24^{Low} populations, indicating the important role of BCSCs in chemotherapy resistance [45]. Hopefully, using anti-BCSC drugs could improve the treatment efficacy. According to a surprising study, as an FDA-approved anthelmintic drug, flubendazole effectively enhanced the antitumor effect when combined with fluorouracil and doxorubicin. Mechanistic studies have shown that flubendazole can significantly reduce the stemness of breast cancer cells [46]. Similarly, the Aurora-A inhibitor AKI603 combined with epirubicin significantly eliminated tumor-initiating cells (TICs) and overcame drug resistance in breast cancer [45]. Interestingly, as a traditional herb derivative from ginseng, Rg3 has different degrees of inhibition of cancer stem-like characteristics via different pathways. For example, Rg3 could block NF- κ B-mediated epithelial-mesenchymal transition and stemness to sensitize lung cancer cells to cisplatin [47]. In addition, Rg3 attenuates the expression of Sox-2 and Bmi-1 mainly through the nuclear localization of Akt-mediat-

ed hypoxia inducible factor-1 α (HIF-1 α) in breast cancer cells [48]. To further explore the underlying mechanism of the anti-BCSC effect of Rg3, we treated breast cancer cells with Rg3 at a given concentration. As expected, Rg3 suppressed mammosphere formation, decreased cancer stem-related marker levels, and reduced ALDH(+) subpopulation numbers (**Figure 2A-F**, [Supplementary Figure 2A-E](#)). Moreover, Rg3 inhibited tumor growth and restrained tumor-initiating frequencies in vivo (**Figure 3A**, **3B** and **3F**). It was shown that as few as 1×10^3 MDA-MB-231 cells could reach a 60% tumor graft rate (3/5 sites), whereas tumor-bearing mice that were intraperitoneally injected with Rg3 achieved a 40% tumor graft rate (2/5 sites) with up to 1×10^4 MDA-MB-231 cells (**Figure 3F**).

As one of the main cancer stem cell reprogramming factors, MYC plays a unique role in tumor initiation [49]. Consistent with these findings, our results showed that MYC depletion in breast cancer cells suppressed mammosphere formation and colony formation compared with those in negative control cells. Surprisingly, there was no significant change in sphere formation or colony formation capacity when we cultured MYC-downregulated cells with Rg3 (**Figure 4B** and **4C**, [Supplementary Figure 3A](#) and [3B](#)). These results indicated that Rg3 depressed BCSCs mainly through downregulating MYC expression. Indeed, overexpression of MYC enhanced the stem-like properties of breast cancer cells, which was dramatically inhibited by Rg3 treatment (**Figure 4E**, **4F**, [Supplementary Figure 3C](#) and [3D](#)). In an effort to investigate the mechanisms underlying the regulation of MYC expression by Rg3, we also detected MYC mRNA expression after Rg3 treatment. As shown in **Figure 3I** and **3J**, we found that Rg3 was likely to decrease MYC mRNA expression at the posttranscriptional level rather than through promoting its transcriptional activity ([Supplementary Figure 4A](#) and [4B](#)). Two regions within MYC mRNAs affect the short half-life of MYC. One is in the 3'-untranslated region (UTR), named the AU-rich element (AURE), and the other is an ~250 nt coding region instability determinant (CRD) in the coding region [50]. The RNA-binding protein HUR can recruit let-7 miRNA to the MYC 3'UTR and promote let-7-loaded RNA-induced silencing complex (RISC) [19]. Notably, let-7 is a conserved microRNA that functions as a tumor suppressor that can inhibit MYC [51]. In our

Rg3 impairs MYC mRNA stability to inhibit breast cancer stemness

study, we found that culture of breast cancer cells with Rg3 significantly shortened the half-life of MYC mRNA (**Figure 5A-D**), indicating a role for Rg3 in destabilizing MYC mRNA. Furthermore, we revealed that the let7 family members, especially let7a and let7b, act as key effectors in the regulation of MYC mRNA stability after Rg3 treatment (**Figure 5E-J**, **Supplementary Figure 4E** and **4F**). Consistently, the protein levels of DICER and RAS, which are targeted by let-7, were increased (**Supplementary Figure 4C** and **4D**).

In conclusion, our findings demonstrate that the traditional Chinese herbal medicine ginsenoside Rg3 has the potential to suppress breast cancer stem-like properties by destabilizing MYC mRNA at the posttranscriptional level. The multifaceted actions of Rg3, observed in both in vitro and in vivo settings, render it a promising and viable therapeutic strategy for the treatment of breast cancer. These preclinical insights provide a strong foundation for future clinical investigations and potential integration of Rg3 into breast cancer therapy protocols.

Acknowledgements

The work was supported by Wu Jieping Medical Foundation (No. 320.6750.2022.03.35). We thank Dr. Bin Qiao for editing the manuscript.

Disclosure of conflict of interest

None.

Address correspondence to: Ju-Hong Wang, Department of Thoracic Surgery, National Cancer Center/National Clinical Research Center for Cancer/Cancer Hospital, Chinese Academy of Medical Sciences and Peking Union Medical College, Beijing 100021, China. E-mail: wjh4028-26@163.com; Xu Zhang, Department of Thoracic Surgery, The Second Hospital of Dalian Medical University Cardiovascular Hospital, No. 50 North Section of Digital Road, Dalian 116000, Liaoning, China. E-mail: zzhangxu0417@163.com; Yi Zhao, Department of Oncology, The First Affiliated Hospital of Dalian Medical University, Dalian Medical University, No. 222, Zhongshan Road, Dalian 116011, Liaoning, China. E-mail: zhaoyi0411@outlook.com

References

[1] Bray F, McCarron P and Parkin DM. The changing global patterns of female breast cancer in-

cidence and mortality. *Breast Cancer Res* 2004; 6: 229-239.

- [2] Dandawate PR, Subramaniam D, Jensen RA and Anant S. Targeting cancer stem cells and signaling pathways by phytochemicals: novel approach for breast cancer therapy. *Semin Cancer Biol* 2016; 40-41: 192-208.
- [3] Filipova A, Seifrtova M, Mokry J, Dvorak J, Rezacova M, Filip S and Diaz-Garcia D. Breast cancer and cancer stem cells: a mini-review. *Tumori* 2014; 100: 363-369.
- [4] Nigam A. Breast cancer stem cells, pathways and therapeutic perspectives 2011. *Indian J Surg* 2013; 75: 170-180.
- [5] Reya T, Morrison SJ, Clarke MF and Weissman IL. Stem cells, cancer, and cancer stem cells. *Nature* 2001; 414: 105-111.
- [6] Ginestier C, Hur MH, Charafe-Jauffret E, Monville F, Dutcher J, Brown M, Jacquemier J, Viens P, Kleer CG, Liu S, Schott A, Hayes D, Birnbaum D, Wicha MS and Dontu G. ALDH1 is a marker of normal and malignant human mammary stem cells and a predictor of poor clinical outcome. *Cell Stem Cell* 2007; 1: 555-567.
- [7] Al-Hajj M, Wicha MS, Benito-Hernandez A, Morrison SJ and Clarke MF. Prospective identification of tumorigenic breast cancer cells. *Proc Natl Acad Sci U S A* 2003; 100: 3983-8.
- [8] Iqbal J, Chong PY and Tan PH. Breast cancer stem cells: an update. *J Clin Pathol* 2013; 66: 485-90.
- [9] Lawson DA, Bhakta NR, Kessenbrock K, Prummel KD, Yu Y, Takai K, Zhou A, Eyob H, Balakrishnan S, Wang CY, Yaswen P, Goga A and Werb Z. Single-cell analysis reveals a stem-cell program in human metastatic breast cancer cells. *Nature* 2015; 526: 131-5.
- [10] Ye X, Tam WL, Shibue T, Kaygusuz Y, Reinhardt F, Ng Eaton E and Weinberg RA. Distinct EMT programs control normal mammary stem cells and tumour-initiating cells. *Nature* 2015; 525: 256-260.
- [11] Seino S, Shigeishi H, Hashikata M, Higashikawa K, Tobiume K, Uetsuki R, Ishida Y, Sasaki K, Naruse T, Rahman MZ, Ono S, Simasue H, Ohta K, Sugiyama M and Takechi M. CD44(high)/ALDH1(high) head and neck squamous cell carcinoma cells exhibit mesenchymal characteristics and GSK3 β -dependent cancer stem cell properties. *J Oral Pathol Med* 2016; 45: 180-8.
- [12] Ponti D, Costa A, Zaffaroni N, Pratesi G, Petrangolini G, Coradini D, Pilotti S, Pierotti MA and Daidone MG. Isolation and in vitro propagation of tumorigenic breast cancer cells with stem/progenitor cell properties. *Cancer Res* 2005; 65: 5506-11.
- [13] Beroukhi R, Mermel CH, Porter D, Wei G, Raychaudhuri S, Donovan J, Barretina J,

Rg3 impairs MYC mRNA stability to inhibit breast cancer stemness

- Boehm JS, Dobson J, Urashima M, Mc Henry KT, Pinchback RM, Ligon AH, Cho YJ, Haery L, Greulich H, Reich M, Winckler W, Lawrence MS, Weir BA, Tanaka KE, Chiang DY, Bass AJ, Loo A, Hoffman C, Prensner J, Liefeld T, Gao Q, Yecies D, Signoretti S, Maher E, Kaye FJ, Sasaki H, Tepper JE, Fletcher JA, Tabernero J, Baselga J, Tsao MS, Demichelis F, Rubin MA, Janne PA, Daly MJ, Nucera C, Levine RL, Ebert BL, Gabriel S, Rustgi AK, Antonescu CR, Ladanyi M, Letai A, Garraway LA, Loda M, Beer DG, True LD, Okamoto A, Pomeroy SL, Singer S, Golub TR, Lander ES, Getz G, Sellers WR and Meyerson M. The landscape of somatic copy-number alteration across human cancers. *Nature* 2010; 463: 899-905.
- [14] Land H, Parada LF and Weinberg RA. Tumorigenic conversion of primary embryo fibroblasts requires at least two cooperating oncogenes. *Nature* 1983; 304: 596-602.
- [15] Park S, Chung S, Kim KM, Jung KC, Park C, Hahm ER and Yang CH. Determination of binding constant of transcription factor myc-max/max-max and E-box DNA: the effect of inhibitors on the binding. *Biochim Biophys Acta* 2004; 1670: 217-228.
- [16] Dang CV. MYC on the path to cancer. *Cell* 2012; 149: 22-35.
- [17] Chang TC, Yu D, Lee YS, Wentzel EA, Arking DE, West KM, Dang CV, Thomas-Tikhonenko A and Mendell JT. Widespread microRNA repression by Myc contributes to tumorigenesis. *Nat Genet* 2008; 40: 43-50.
- [18] O'Donnell KA, Wentzel EA, Zeller KI, Dang CV and Mendell JT. c-Myc-regulated microRNAs modulate E2F1 expression. *Nature* 2005; 435: 839-43.
- [19] Kim HH, Kuwano Y, Srikantan S, Lee EK, Martindale JL and Gorospe M. HuR recruits let-7/RISC to repress c-Myc expression. *Genes Dev* 2009; 23: 1743-1748.
- [20] Christoffersen NR, Shalgi R, Frankel LB, Leucci E, Lees M, Klausen M, Pilpel Y, Nielsen FC, Oren M and Lund AH. p53-independent upregulation of miR-34a during oncogene-induced senescence represses MYC. *Cell Death Differ* 2010; 17: 236-245.
- [21] Sachdeva M, Zhu S, Wu F, Wu H, Walia V, Kumar S, Elble R, Watabe K and Mo YY. p53 represses c-Myc through induction of the tumor suppressor miR-145. *Proc Natl Acad Sci U S A* 2009; 106: 3207-3212.
- [22] Laurenti E, Wilson A and Trumpp A. Myc's other life: stem cells and beyond. *Curr Opin Cell Biol* 2009; 21: 844-854.
- [23] Takahashi K and Yamanaka S. Induction of pluripotent stem cells from mouse embryonic and adult fibroblast cultures by defined factors. *Cell* 2006; 126: 663-676.
- [24] Li Y, Wang Y, Niu K, Chen X, Xia L, Lu D, Kong R, Chen Z, Duan Y and Sun J. Clinical benefit from EGFR-TKI plus ginsenoside Rg3 in patients with advanced non-small cell lung cancer harboring EGFR active mutation. *Oncotarget* 2016; 7: 70535-70545.
- [25] Park EH, Kim YJ, Yamabe N, Park SH, Kim HK, Jang HJ, Kim JH, Cheon GJ, Ham J and Kang KS. Stereospecific anticancer effects of ginsenoside Rg3 epimers isolated from heat-processed American ginseng on human gastric cancer cell. *J Ginseng Res* 2014; 38: 22-7.
- [26] Shan X, Fu YS, Aziz F, Wang XQ, Yan Q and Liu JW. Ginsenoside Rg3 inhibits melanoma cell proliferation through down-regulation of histone deacetylase 3 (HDAC3) and increase of p53 acetylation. *PLoS One* 2014; 9: e115401.
- [27] Tian L, Shen D, Li X, Shan X, Wang X, Yan Q and Liu J. Ginsenoside Rg3 inhibits epithelial-mesenchymal transition (EMT) and invasion of lung cancer by down-regulating FUT4. *Oncotarget* 2016; 7: 1619-1632.
- [28] Kim BM, Kim DH, Park JH, Surh YJ and Na HK. Ginsenoside Rg3 inhibits constitutive activation of NF- κ B signaling in human breast cancer (MDA-MB-231) cells: ERK and Akt as potential upstream targets. *J Cancer Prev* 2014; 19: 23-30.
- [29] Kim JW, Jung SY, Kwon YH, Lee JH, Lee YM, Lee BY and Kwon SM. Ginsenoside Rg3 attenuates tumor angiogenesis via inhibiting bioactivities of endothelial progenitor cells. *Cancer Biol Ther* 2012; 13: 504-515.
- [30] Kim DG, Jung KH, Lee DG, Yoon JH, Choi KS, Kwon SW, Shen HM, Morgan MJ, Hong SS and Kim YS. 20(S)-ginsenoside Rg3 is a novel inhibitor of autophagy and sensitizes hepatocellular carcinoma to doxorubicin. *Oncotarget* 2014; 5: 4438-4451.
- [31] Liu TG, Huang Y, Cui DD, Huang XB, Mao SH, Ji LL, Song HB and Yi C. Inhibitory effect of ginsenoside Rg3 combined with gemcitabine on angiogenesis and growth of lung cancer in mice. *BMC Cancer* 2009; 9: 250.
- [32] Pu H, Zheng Q, Li H, Wu M, An J, Gui X, Li T and Lu D. CUDR promotes liver cancer stem cell growth through upregulating TERT and C-Myc. *Oncotarget* 2015; 6: 40775-40798.
- [33] Kuo HY, Hsu HT, Chen YC, Chang YW, Liu FT and Wu CW. Galectin-3 modulates the EGFR signalling-mediated regulation of Sox2 expression via c-Myc in lung cancer. *Glycobiology* 2016; 26: 155-165.
- [34] Büssing I, Slack FJ and Grosshans H. Let-7 microRNAs in development, stem cells and cancer. *Trends Mol Med* 2008; 14: 400-409.
- [35] Heo I, Joo C, Kim YK, Ha M, Yoon MJ, Cho J, Yeom KH, Han J and Kim VN. TUT4 in concert with Lin28 suppresses microRNA biogenesis

Rg3 impairs MYC mRNA stability to inhibit breast cancer stemness

- through pre-microRNA uridylation. *Cell* 2009; 138: 696-708.
- [36] Tacar O, Sriamornsak P and Dass CR. Doxorubicin: an update on anticancer molecular action, toxicity and novel drug delivery systems. *J Pharm Pharmacol* 2013; 65: 157-170.
- [37] Kwon WS, Rha SY, Jeung HC, Kim TS and Chung HC. Modulation of HAT activity by the BRCA2 N372H variation is a novel mechanism of paclitaxel resistance in breast cancer cell lines. *Biochem Pharmacol* 2017; 138: 163-173.
- [38] Slamon DJ, Clark GM, Wong SG, Levin WJ, Ullrich A and McGuire WL. Human breast cancer: correlation of relapse and survival with amplification of the HER-2/neu oncogene. *Science* 1987; 235: 177-182.
- [39] Paik S, Bryant J, Tan-Chiu E, Yothers G, Park C, Wickerham DL and Wolmark N. HER2 and choice of adjuvant chemotherapy for invasive breast cancer: national surgical adjuvant breast and bowel project protocol B-15. *J Natl Cancer Inst* 2000; 92: 1991-1998.
- [40] Wege AK, Weber F, Kroemer A, Ortmann O, Nimmerjahn F and Brockhoff G. IL-15 enhances the anti-tumor activity of trastuzumab against breast cancer cells but causes fatal side effects in humanized tumor mice (HTM). *Oncotarget* 2017; 8: 2731-2744.
- [41] Sun Y, Lin H, Zhu Y, Feng J, Chen Z, Li G, Zhang X, Zhang Z, Tang J, Shi M, Hao X and Han H. A randomized, prospective, multi-centre clinical trial of NP regimen (vinorelbine+cisplatin) plus Gensing Rg3 in the treatment of advanced non-small cell lung cancer patients. *Zhongguo Fei Ai Za Zhi* 2006; 9: 254-258.
- [42] Chen D, Zhao Y, Bai S, Shi Z and Zhang J. Effect of ginsenoside Rg3 on the progression of orthotopically xenotransplanted human breast cancer in nude mice and its mechanism. *Sichuan Da Xue Xue Bao Yi Xue Ban* 2003; 34: 546-548.
- [43] Zhang Y, Liu QZ, Xing SP and Zhang JL. Inhibiting effect of Endostar combined with ginsenoside Rg3 on breast cancer tumor growth in tumor-bearing mice. *Asian Pac J Trop Med* 2016; 9: 180-183.
- [44] Xu LZ, Li SS, Zhou W, Kang ZJ, Zhang QX, Kamran M, Xu J, Liang DP, Wang CL, Hou ZJ, Wan XB, Wang HJ, Lam EW, Zhao ZW and Liu Q. p62/SQSTM1 enhances breast cancer stem-like properties by stabilizing MYC mRNA. *Oncogene* 2017; 36: 304-317.
- [45] Zheng FM, Long ZJ, Hou ZJ, Luo Y, Xu LZ, Xia JL, Lai XJ, Liu JW, Wang X, Kamran M, Yan M, Shao SJ, Lam EW, Wang SW, Lu G and Liu Q. A novel small molecule aurora kinase inhibitor attenuates breast tumor-initiating cells and overcomes drug resistance. *Mol Cancer Ther* 2014; 13: 1991-2003.
- [46] Hou ZJ, Luo X, Zhang W, Peng F, Cui B, Wu SJ, Zheng FM, Xu J, Xu LZ, Long ZJ, Wang XT, Li GH, Wan XY, Yang YL and Liu Q. Flubendazole, FDA-approved anthelmintic, targets breast cancer stem-like cells. *Oncotarget* 2015; 6: 6326-6340.
- [47] Wang J, Tian L, Khan MN, Zhang L, Chen Q, Zhao Y, Yan Q, Fu L and Liu J. Ginsenoside Rg3 sensitizes hypoxic lung cancer cells to cisplatin via blocking of NF- κ B mediated epithelial-mesenchymal transition and stemness. *Cancer Lett* 2018; 415: 73-85.
- [48] Oh J, Yoon HJ, Jang JH, Kim DH and Surh YJ. The standardized Korean Red Ginseng extract and its ingredient ginsenoside Rg3 inhibit manifestation of breast cancer stem cell-like properties through modulation of self-renewal signaling. *J Ginseng Res* 2019; 43: 421-430.
- [49] Loi S, Haibe-Kains B, Majjaj S, Lallemand F, Durbecq V, Larsimont D, Gonzalez-Angulo AM, Pusztai L, Symmans WF, Bardelli A, Ellis P, Tutt AN, Gillett CE, Hennessy BT, Mills GB, Phillips WA, Piccart MJ, Speed TP, McArthur GA and Sotiriou C. PIK3CA mutations associated with gene signature of low mTORC1 signaling and better outcomes in estrogen receptor-positive breast cancer. *Proc Natl Acad Sci U S A* 2010; 107: 10208-10213.
- [50] Doyle GA, Betz NA, Leeds PF, Fleisig AJ, Prokipcak RD and Ross J. The c-myc coding region determinant-binding protein: a member of a family of KH domain RNA-binding proteins. *Nucleic Acids Res* 1998; 26: 5036-5044.
- [51] Chien CS, Wang ML, Chu PY, Chang YL, Liu WH, Yu CC, Lan YT, Huang PI, Lee YY, Chen YW, Lo WL and Chiou SH. Lin28B/let-7 regulates expression of Oct4 and Sox2 and reprograms oral squamous cell carcinoma cells to a stem-like state. *Cancer Res* 2015; 75: 2553-2565.

Rg3 impairs MYC mRNA stability to inhibit breast cancer stemness

Supplementary Materials and Methods

Cell viability assay and colony formation assay

For cell viability assay, cells were plated at a density of 1,000 cells/well in 96-well plates. The cytotoxic effect of 20 (R)-Rg3 was evaluated in different time point or concentration using cell counting assay kit-8 (CCK-8) according to the manufacturer's instructions (CCK-8, Beyotime, Shanghai, China). For colony formation assay, dissociated 1,000 cells were seeded in 6-cm dishes and treated with indicated concentration of 20 (R)-Rg3 for 2 weeks. After being cultured, cells were fixed and stained with 1% crystal violet (Shanghai Sengon Company, Shanghai, China) for 10 min at room temperature, then washed with phosphate buffered saline (PBS, Shanghai Sengon Company, Shanghai, China). The number of colonies, defined as >50 μm cells/colony were counted. Triplicate dishes were set up.

Western blot

After incubated with varying concentration of Rg3 for different times, cells were harvested and lysed in RIPA buffer containing 50 mM Tris pH 7.4, 150 mM NaCl, 1% NP-40, 0.5% sodium deoxycholate, 0.1% SDS, 1 mM phenylmethyl sulfonyl fluoride with freshly added cocktail protease inhibitor. Equal amounts of protein extract were separated by SDS-PAGE gel electrophoresis and transferred to a NC membrane (Millipore). The membranes were blocked with 5% fat-free milk in TBST at room temperature for 1 hour and incubated at 4°C overnight with primary antibodies, followed by incubation with peroxidase-conjugated secondary antibodies (Thermo Scientific, Rockford, IL, USA) for one hour at room temperature. Proteins were visualized by chemiluminescence (Amersham, Marlborough, MA, USA). The Primary antibodies were used as follows: β -actin (Proteintech, Wuhan, China), c-Myc (Cell Signaling Technology, Danvers, MA, USA), SOX2 (Cell Signaling Technology, Danvers, MA, USA), OCT4 (Cell Signaling Technology, Danvers, MA, USA), LIN28 (Abcam, Cambridge, MA, USA), DICER (Cell Signaling Technology, Danvers, MA, USA) and RAS (Cell Signaling Technology, Danvers, MA, USA).

ALDH sorting assay

The ALDEFLUOR kit (Shanghai Stem Cell Technology Co. Ltd, Shanghai, China) was used for isolating the population with a high ALDH enzymatic activity. Cells which were exposed to Rg3 (25 μM) for 72 h were trypsinized, washed twice with PBS, then cells were suspended in ALDEFLUOR assay buffer containing ALDH substrate (BAAA, 1 $\mu\text{mol/l}$ per 1×10^6 cells) and incubated for 45 minutes at 37°C. As negative controls, for each sample of cells an aliquot was treated with 50 mmol/L diethylaminobenzaldehyde (DEAB), a specific ALDH inhibitor. The ALDH-positive subpopulation was analyzed by BD FACS calibur flow cytometer.

RNA extraction, miRNA extraction, reverse transcription-PCR and quantitative real-time PCR

Total RNA was extracted from breast cancer cells using the Trizol reagent (Invitrogen, Carlsbad, CA, USA) following manufacturer's instructions. The cDNA was generated with an oligo-dT primer by using SuperScript III RT System (TransGene Biotech, Beijing, China). Quantitative real-time PCR (RT-qPCR) was performed using Platinum SYBR Green QPCR SuperMix (Invitrogen, Carlsbad, CA, USA) as recommended by the manufacturer. Changes of mRNA levels were determined by the $2^{-\Delta\Delta\text{CT}}$ method using Actin for internal crossing normalization. Detailed primer sequences for qPCR were listed in [Supplementary Table 1](#).

Supplementary Table 1. Detailed primer sequences for qPCR

Gene name	5' -> 3'
let-7a	AACUAUACAACCUACUACCUCA
let-7b	AACCACACAACCUACUACCUCA

Rg3 impairs MYC mRNA stability to inhibit breast cancer stemness

For miRNA extraction, total RNAs were extracted from breast cancer cells using miRNeasy Mini kit (Qiagen, 217004, Germany). Levels of mature miRNAs were determined by RT-qPCR using miScript reverse transcription kit (Qiagen, 218061, Germany) and miScript SYBR Green PCR kit (Qiagen, 218073, Germany) according to the manufacturers' instructions. PCR primer sets specific for let-7 were used with miScript Primer Assays (Qiagen, MS00006482, MS00003122, MS00003129, MS00031227, MS00006489, MS00008337, Germany), and the indicated miRNA levels were normalized against snRNA RNU6B.

Lentivirus preparation and infection

HEK293T cells were used for packaging lentivirus with the 2nd generation packaging system plasmid psPAX2 (Addgene, Cambridge, MA, USA) and pMD2.G (Addgene, Cambridge, MA, USA). For infection with the lentivirus, cells were infected in 6-well plates and subsequently split into 10 cm dishes in the presence of 2 µg/mL puromycin (Sigma, St Louis, MO, USA) for selection over 72 hours.

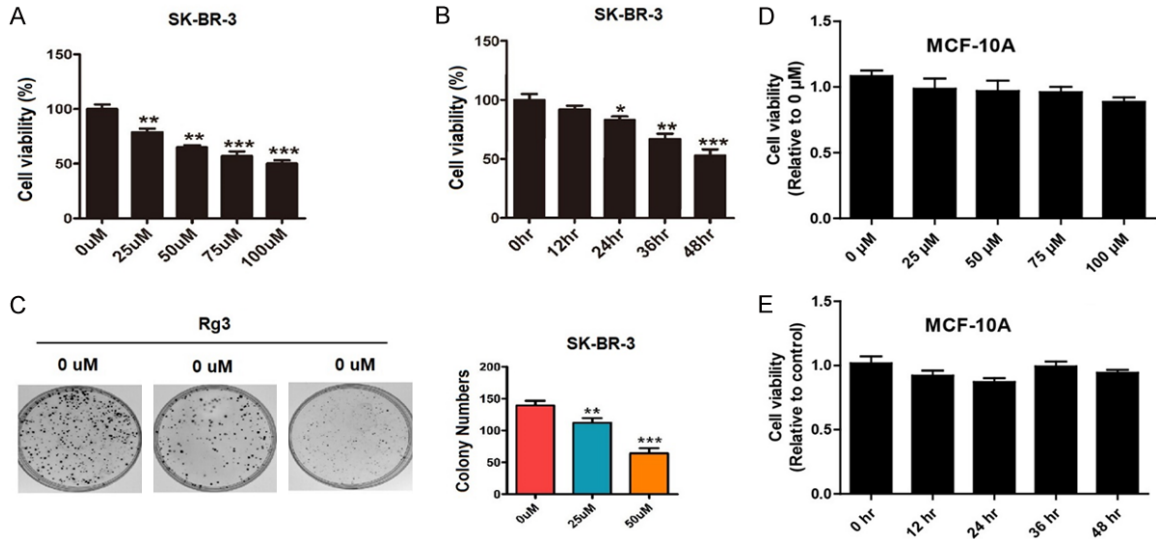
Plasmids

Promoters of MYC (-2,269/+516) was amplified from MDA-MB-231 genomic DNA and inserted into pGL3-Basic (Promega, Madison, WI, USA) to construct pGL3-MYC. Primers were as follows: 5' MluI, 5'-CGACGCGTCGGCCACCGGGAGAGAAAAGTTTACT; 3'HindIII, 5'-CCCAAGCTTGGGCTGGTTTTCCACTACCG. The full-length MYC plasmid, shRNA targeting MYC (shMYC-1, shMYC-2) and the non-target shRNA were kindly provided by Dr Si-Si Li (Institute of Cancer Stem Cell, Dalian Medical University, Dalian, China) and packaged for lentivirus particles.

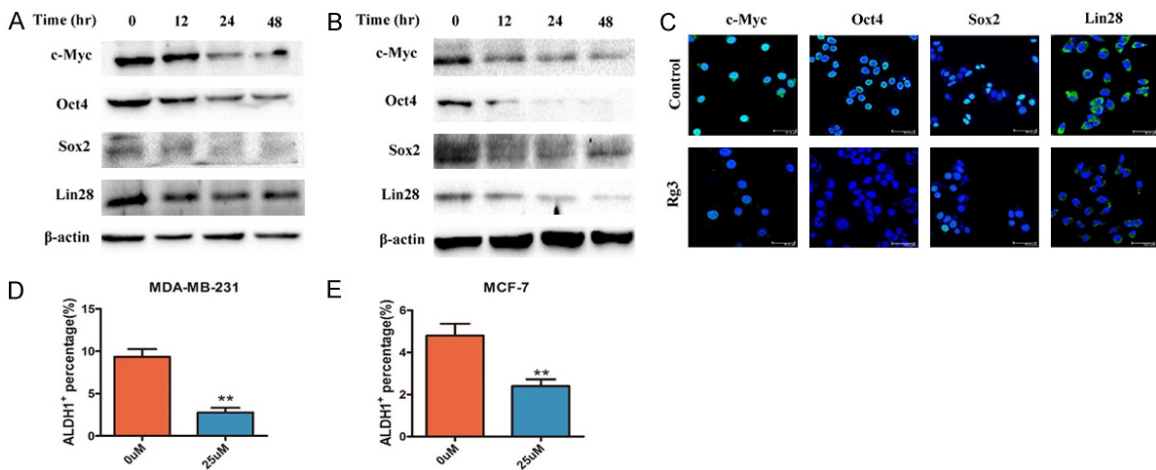
Dual-luciferase reporter assay

For dual-luciferase reporter assay, MDA-MB-231 and MCF-7 cells were seeded into 12-well plates at the confluence of 70%. Next, cells were cultured with or without Rg3 (50 µM) and were transiently cotransfected with pGL3-MYC reporter construct or empty pGL3-basic vector and phRL-TK Renilla control plasmid by using Lipofectamine 2000 (Invitrogen, Carlsbad, CA, USA). After transfection, luciferase activity was measured using the Dual-Luciferase Reporter Assay System Kit (Promega, Beijing, China) according to the manufacturer's instructions. Growth media were removed and cells were washed with PBS. Passive lysis buffer 500 µl per well was added with gentle rocking for 15 min at room temperature. Ten microlitres of lysate were transferred in black 96-well plate. For each luminescence reading, there would be a 2-s pre-measurement delay after injector dispensing assay reagents into each well, followed by a 10-s measurement time. Luciferase activity was quantified with a luminometer (Molecular Devices, Sunnyvale, San Francisco, USA). Transcription activity was calculated as the ratio of Firefly luciferase activity (reporter) v.s. Renilla luciferase activity (control). All data were analyzed from at least three independent experiments.

Rg3 impairs MYC mRNA stability to inhibit breast cancer stemness

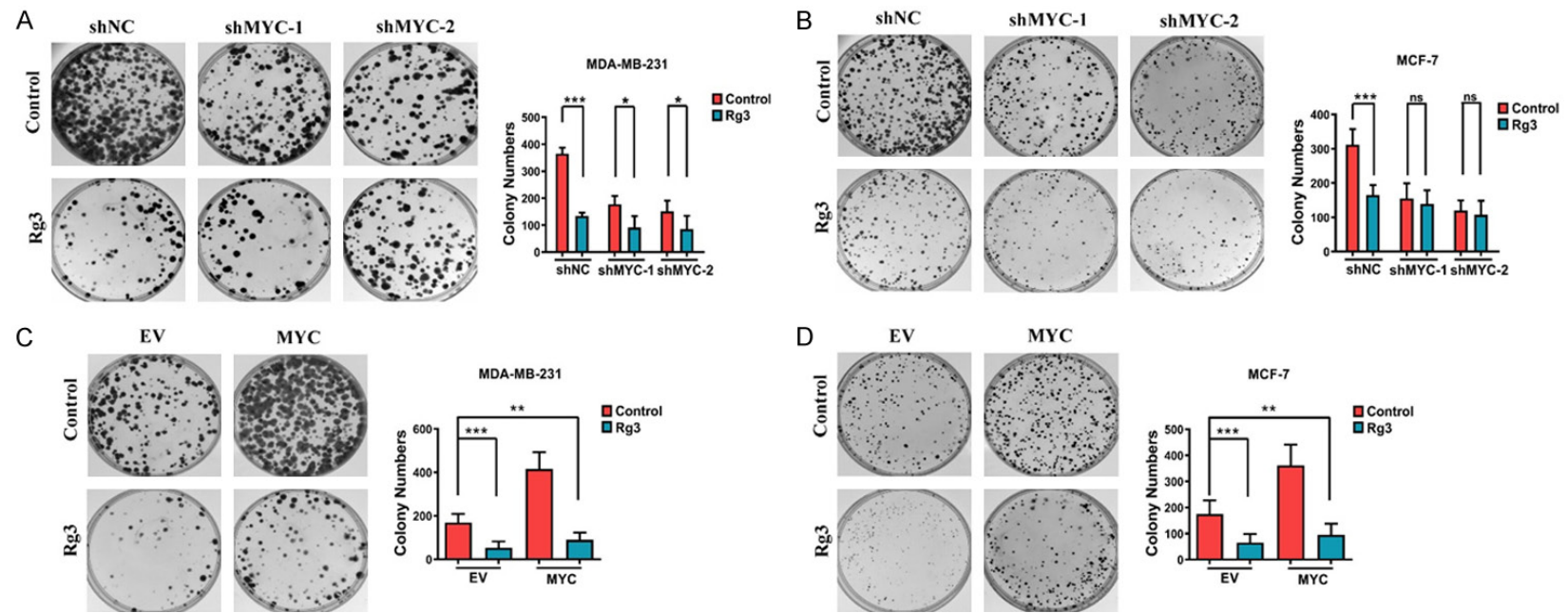


Supplementary Figure 1. A. SK-BR-3 cells were treated with Rg3 (0 μ M, 25 μ M, 50 μ M, 100 μ M) for 48 h. Cell viability was determined by a CCK-8 assay as described in the Materials and Methods. B. SK-BR-3 cells were treated with 50 μ M Rg3 for 0 h, 12 h, 24 h, 36 h, or 48 h. Cell viability was determined by a CCK-8 assay. C. Plate colony formation was analyzed following treatment with different concentrations of Rg3 (0 μ M, 25 μ M, 50 μ M) in SK-BR-3 cells. D. MCF-10A cells were treated with Rg3 (0 μ M, 25 μ M, 50 μ M, 100 μ M) for 48 h. Cell viability was determined by a CCK-8 assay as described in the Materials and Methods. E. MCF-10A cells were treated with 50 μ M Rg3 for 0 h, 12 h, 24 h, 36 h, or 48 h. Cell viability was determined by a CCK-8 assay. The data are presented as the mean \pm SD of three independent experiments. Comparisons were analyzed by two-tailed Student's t tests. * P < 0.05, ** P < 0.01, *** P < 0.001.



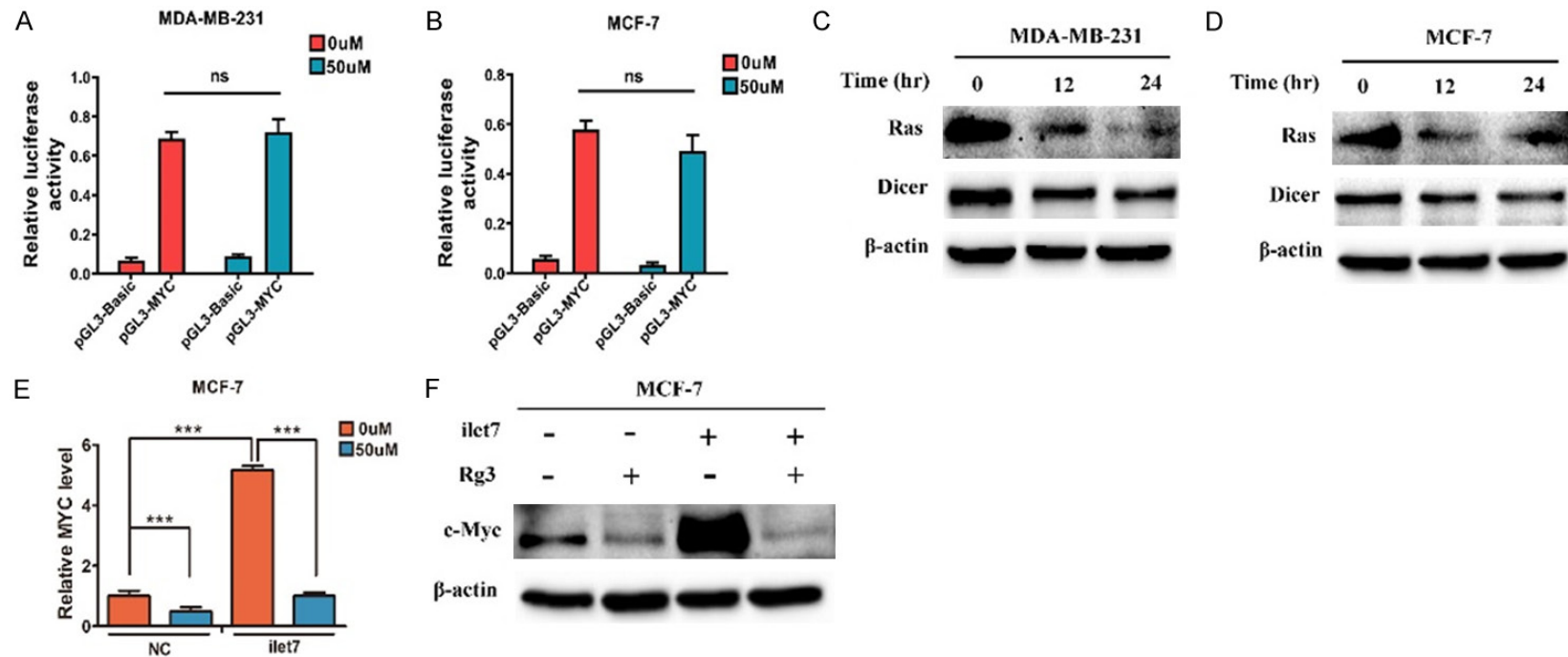
Supplementary Figure 2. (A) The expression of c-Myc, Oct4, Sox2, and Lin28 in MDA-MB-231 cells and (B) MCF-7 cells was analyzed after treatment with 50 μ M Rg3 for 0 h, 12 h, 24 h, 36 h, or 48 h by western blot. MDA-MB-231 cells were treated with 50 μ M Rg3 for 0, 12, 24, 36, or 48 h. (C) Immunofluorescence staining of c-Myc, Oct4, Sox2, and Lin28 in MDA-MB-231 cells with or without Rg3 treatment. DAPI was used for nuclear staining. (D) Column graph showing ALDH-positive populations in MDA-MB-231 cells and (E) MCF-7 cells treated with different concentrations of Rg3 (0 μ M, 25 μ M). The data are presented as the mean \pm SD of three independent experiments. Comparisons were analyzed by two-tailed Student's t tests. * P < 0.05, ** P < 0.01, *** P < 0.001. Scale bars, 500 μ m.

Rg3 impairs MYC mRNA stability to inhibit breast cancer stemness



Supplementary Figure 3. (A) Comparisons of colony formation were performed following decreases in MYC expression in MDA-MB-231 cells and (B) MCF-7 cells. (C) Comparisons of colony formation were performed following increases in MYC expression in MDA-MB-231 cells and (D) MCF-7 cells. The data are presented as the mean \pm SD of three independent experiments. Comparisons were analyzed by two-tailed Student's t tests. * $P < 0.05$, ** $P < 0.01$, *** $P < 0.001$.

Rg3 impairs MYC mRNA stability to inhibit breast cancer stemness



Supplementary Figure 4. (A) The full-length MYC promoter sequence was cloned and inserted into the pGL3-Basic plasmid, and dual-luciferase assays were performed in MDA-MB-231 cells and (B) MCF-7 cells with or without Rg3, as described in [Supplementary Materials and Methods](#). Transcription activity was calculated as the ratio of firefly luciferase activity (reporter) to Renilla luciferase activity (control). (C) MDA-MB-231 and (D) MCF-7 cells were cultured with Rg3. The cells were then harvested and subjected to western blotting. RAS and DICER abundances were used to evaluate the working efficiency of the let-7 cluster. (E) MCF-7 cells were treated with the let-7a/b inhibitor with or without Rg3. The relative MYC concentration was measured by RT-qPCR. (F) MCF-7 cells were treated with the let-7a/b inhibitor with or without Rg3. The protein expression of c-Myc was measured by western blotting. The data are presented as the mean \pm SD of three independent experiments. Comparisons were analyzed by two-tailed Student's t tests. ns means not significant. *P < 0.05, **P < 0.01, ***P < 0.001.